Available online at www.sciencedirect.com
ScienceDirect
Journal of Magnetic Resonance 187 (2007) 225–233
JMR Journal of Magnetic Resonance
www.elsevier.com/locate/jmr

A new decoupling method for accurate quantification of polyethylene copolymer composition and triad sequence distribution with ^{13}C NMR

Zhe Zhou [a,*], Rainer Kümmerle [b,*], Xiaohua Qiu [c], David Redwine [c], Rongjuan Cong [a], Angela Taha [a], Dan Baugh [a], Bill Winniford [a]

[a] The Dow Chemical Company, 2301 N. Brazosport Blvd., Freeport, TX 77541, USA
[b] Bruker BioSpin AG, NMR division, Industriestrasse 26, CH-8117 Fällanden, Switzerland
[c] The Dow Chemical Company, Midland, MI 48667, USA

Received 3 April 2007; revised 4 May 2007
Available online 23 May 2007

Abstract

^{13}C NMR is a powerful analytical tool for characterizing polyethylene copolymer composition and sequence distribution. Accurate characterization of the composition and sequence distribution is critical for researchers in industry and academia. Some common composite pulse decoupling (CPD) sequences used in polyethylene copolymer ^{13}C NMR can lead to artifacts such as modulations of the decoupled ^{13}C NMR signals (decoupling sidebands) resulting in systematic errors in quantitative analysis. A new CPD method was developed, which suppresses decoupling sidebands below the limit of detection (less than 1:40,000 compared to the intensity of the decoupled signal). This new CPD sequence consists of an improved Waltz-16 CPD, implemented as a bilevel method. Compared with other conventional CPD programs this new decoupling method produced the cleanest ^{13}C NMR spectra for polyethylene copolymer composition and triad sequence distribution analyses.

Keywords: NMR; Polyethylene copolymer; Composition and sequence distribution; Composite pulse decoupling; Decoupling sidebands; Waltz; Bilevel

1. Introduction

^{13}C NMR is a primary analytical tool for characterizing polyethylene copolymer composition and triad sequence distribution [1–4]. The polyethylene copolymer sequence distribution was often characterized with triads since not all tetrads and pentads could be assigned at this time [5].

Accurate characterization of polyethylene copolymer composition and triad sequence distribution is critical for understanding structure–property relationships, developing product specifications and for researchers involved in new product development.

In order to get quantitative ^{13}C NMR, the following criteria are critical: correct transmitter and decoupler offset settings; short enough pulse length for homogeneous excitation; correct digital resolution; recycle time (acquisition time plus pulse delay) typically larger than five times of the longest ^{13}C spin-lattice relaxation time (T_1) in the sample; correct ratio of acquisition to delay time to avoid transient Nuclear Overhauser Effect (NOE); inverse gated decoupling pulse sequences to avoid steady state NOE build up; efficient decoupling with good bandwidth, and finally no decoupling sidebands.

The transmitter frequency should be set near the center of the range of interest and the decoupler offset should be close to the proton signals from the ethylene backbone.

* Corresponding authors. Fax: +1 979 238 0752 (Z. Zhou), +41 44 825 9696 (R. Kümmerle).
E-mail addresses: zzhou@dow.com (Z. Zhou), rainer.kuemmerle@bruker-biospin.ch (R. Kümmerle).

1090-7807/$ - see front matter © 2007 Elsevier Inc. All rights reserved.
doi:10.1016/j.jmr.2007.05.005

The peaks will not be digitized correctly if the digital resolution is too low, on the contrary too much digital resolution will result in excessively long acquisition time, risk of transient NOE and lower signal to noise ratio.

Unless a suitable delay is allowed between hard ^{13}C pulses, the area of the resonance may be either attenuated due to saturation or enhanced due to transient NOE effects [6]. The methyl carbons in a polyethylene copolymer generally have the longest T_1, some of which are as long as 8–10 s. The T_1 of the methylene carbon adjacent to the methyl carbon in poly(ethylene-co-1-octene) (EO) is 7.5 s on a 500 MHz spectrometer. Using the typical five times T_1 as the relaxation delay results in a very long inter pulse delay and long acquisition times. To avoid these problems, a spin relaxation agent (e.g., $Cr(AcAc)_3$ [7–11]) is used to reduce the T_1s. Even with reasonable concentrations of $Cr(AcAc)_3$ (0.05 M), some carbons still have relative long T_1s which are larger than one fifth of the recycle delay. These peaks should not be used for quantitative analysis unless a compensation factor based on data acquired with at least five times of T_1 is used.

Avoidance of NOE is a key concern for the quantitative ^{13}C NMR. Proton decoupling during the relaxation delay can cause saturation of the proton spins coupled to ^{13}C, resulting in enhanced ^{13}C signals. If the NOE ratios were identical for all ^{13}C nuclei in the sample, the peak integrals obtained would all be scaled by the same factor, and quantitative analysis could be performed using spectra acquired with full NOE. Unfortunately, the NOEs vary for different carbons in a polymer [4]. Other ^{13}C relaxation mechanisms, such as chemical shift anisotropy, proton–carbon scalar coupling, dipolar interaction with unpaired electrons of a paramagnetic impurity, can compete with proton-mediated dipolar ^{13}C relaxation and lead to less than full NOE. It should be noted that $Cr(AcAc)_3$ will only attenuate the NOE, but not eliminate NOE with the optimum $Cr(AcAc)_3$ concentration used for polyolefins; therefore it is desirable to use inverse gated decoupling pulse sequences to minimize the NOE. The spectral resolution will decrease significantly if the $Cr(AcAc)_3$ concentration is too high [4].

Since the first introduction of noise modulated decoupling [12], many pulse sequences have been developed to improve the efficiency of heteronuclear decoupling in liquids. For example, decoupling sequences based on composite pulses with phase-modulation, such as Malcolm LEVitt sequences (MLEV) [13–16], Waltz [17,18], and Globally optimized Alternating phase Rectangular Pulse (GARP) [19,20] were proven to be very successful. Adiabatic frequency-sweeping sequences were developed to offer better efficiency of heteronuclear decoupling in order to fulfill the demanding requirement of ultrahigh-field NMR spectrometers [21–24]. Two Pulse Phase Modulation (TPPM) and Small Phase Angle Rapid Cycling (SPARC) decoupling schemes were also developed for solid samples and liquid crystals [25,26]. It is a challenge to obtain high quality spectra and decouple protons in polyethylene copolymers with some common decoupling sequences, such as Waltz-16, when a strong ^{13}C NMR signal such as the main polymethylene resonance of a polyethylene copolymer is present [3]. Decoupling sidebands (cycling sidebands) are observed resulting in spurious peaks and inaccurate integrated intensities. These sidebands result from a periodic modulation of ^{13}C magnetization due to the cyclic nature of multi-pulse proton decoupling methods. These sidebands can present a source of systematic errors in composition and sequence distribution results by distorting the true intensities of the various peaks. Shaka et al.,[17,18,27] Dykstra et al.[28] and Kupce et al.[29] have done excellent work in reducing the decoupling sidebands. Zhang and Gorenstein also improved quality of ^{1}H NMR by reducing adiabatic decoupling sidebands [30]. In this report, the ^{13}C NMR results of two polymer samples using an improved Waltz CPD sequences are shown. The results are compared with Waltz-16, and finally with a bilevel implementation of the improved Waltz CPD sequence. This bilevel CPD decoupling method gives significantly higher quality ^{13}C spectra for polyethylene copolymers.

After acquiring high quality ^{13}C NMR spectra, the next step is analyzing the data to obtain copolymer composition and triad sequence distribution results. Results are presented herein for an EO sample.

2. Experimental section

2.1. Polyolefin sample preparation

Sample A: 0.45 g of high density polyethylene (HDPE) was placed into a Norell 10 mm NMR tube followed by 3 g of 1,1,2,2-tetrachloroethane-d_2/*ortho*-dichlorobenzene (TCE-d_2/ODCB) (w:w, 1:1). Oxygen was reduced by a nitrogen purge via an inserted pipette for ca. 4 min. The tube was capped and placed in an aluminum heating block at 150 °C for several hours. The sample was periodically checked for homogeneity and mixed manually as necessary. A homogeneous mixture was evident by visualization of the uniform distribution of the polymer in solution with no apparent areas of high solvent concentration or air pockets.

Sample B: 0.25 g of EO copolymer sample was added to a Wilmad thin-wall 10 mm NMR tube with 3.2 g of stock solvent, then purged in the N_2 box for 2 h. The stock solvent was made by dissolving 2 g perdeuterated 1,4-dichlorobenzne in 39.2 g ODCB with 0.025 M $Cr(AcAc)_3$. The sample tube was then heated in a heating block at 150 °C. The sample tube was repeatedly vortexed and heated until the solution flows consistently from top of the solution column to the bottom. The sample tube was then left in the heat block for at least 24 h to achieve sample homogenization.

2.2. Waltz CPD sequences modification

The Waltz-16 sequence consists of a repetition of the QQQQ sequence (underlined stands for a 180° phase offset). The basic 9-step Q element consists of the 342312423

Table 1
Different Waltz CPD sequences derived from the original Waltz-16

Waltz-16: QQQQ
Waltz-17: QQQQ + 90°X
Waltz-64: QQQQ QQQQ QQQQ QQQQ
Waltz-65: QQQQ QQQQ QQQQ QQQQ + 90°X

sequence, where 3 denotes a 270° pulse with phase X, 4 denotes a 360° pulse with phase X. The spins undergo a total rotation of 1170–990 = 180° during a Q element. The net rotation for the Waltz-16 supercycle is 0. A first modification of the Waltz-16 CPD sequence consisted in the addition of an additional 90° pulse after each Waltz-16 supercycle, which was called Waltz-17. This introduces a net 90° rotation for the basic Waltz-17 supercycle. The basic super cycle of the Waltz-16 sequence was then modified by implementing a MLEV-4 supercycle, leading to the Waltz-64 CPD sequence. The total spin rotation is still maintained at 0. In a second step, a 90° pulse was added at the end of the Waltz-64 supercycle, leading to the Waltz-65 CPD sequence. This introduces a net 90° rotation of the spins within each Waltz-65 supercycle (Table 1).

2.3. Experimental parameters influencing decoupling sidebands

Decoupling sidebands are modulations of the decoupled NMR signals, which arise due to the cyclic behavior of most CPD sequences, even if applied in an asynchronous way. The frequencies of the decoupling sidebands depend on the CPD sequence as well as on the basic CPD pulse length employed (as this will define the length of the periodicity). The choice of the CPD sequence will also influence the intensity of the decoupling sidebands, which are typically in the 1/2000 to 1/50 range compared to the intensity of the decoupled NMR signal. Decoupling sideband intensities depend on many different parameters, some of them not being directly accessible to the NMR spectroscopist, like the B_2 homogeneity of the RF coil used for decoupling. The authors wanted to assess the most prominent user accessible spectroscopic parameters to achieve reduction of the decoupling sideband intensities for a given probe. The influence of the CPD pulse length and power level and the decoupler offset (with respect to the frequency of the decoupled spin) were explored, and the results obtained using various different Waltz CPD sequences were compared.

2.4. Polyolefin ^{13}C NMR

The ^{13}C NMR spectra were acquired on a Bruker 400 MHz spectrometer with a broadband observe probe at 125 ± 0.1 °C. Temperature was calibrated by replacing the NMR sample tube with a tube containing 80% ethylene glycol and 20% DMSO-d_6 at the same sample height as the polymer solution. N_2 gas was used for temperature control and to flush the probe. Elevating sample temperature to 130 °C did not result in improvement of the resolution, but leads to longer T_1s [4]. Sample spinning did not significantly affect the ^{13}C NMR lineshape in the polymer spectra, therefore NMR spectra were obtained without sample spinning [3]. The magnet was carefully shimmed to generate a lineshape of less than 1 Hz linewidth at half height for the two high-field ODCB solvent peaks. Prior to data acquisition, the observe pulse widths were verified for both the ^{13}C and ^{1}H channels by determination of the 90° pulse widths. The center of the spectrum was set at 32.5 ppm with spectrum width set at 250 ppm. Acquisition parameters were 1.3 s acquisition time, a relaxation delay time 6–13.7 s, and 800–8000 scans for data averaging.

3. Results and discussion

3.1. Modified CPD decoupling sequences

CPD decoupling sequences should allow for efficient and complete decoupling over the largest bandwidth possible for a given pulse length/power combination and generate the smallest artifacts. The first check was therefore the residual coupling, as measured by the linewidth at half height, that could be achieved with the different decoupling schemes. Using a ^{13}C lineshape standard sample (40% dioxane in 60% deuterated benzene) the modified Waltz-64 and Waltz-65 showed similar or even slightly smaller residual coupling compared to Waltz-16 CPD decoupling. The use of Waltz-17 CPD decoupling produced slightly broader lines than Waltz-16 (data not shown). Second, the decoupling profiles at 2.5 and 3.125 kHz decoupling field strength were acquired to compare the different CPD schemes. In order to keep the acquisition time at reasonable levels, ^{13}C enriched MeOH sample with $GdCl_3$ as relaxation agent was used. The results are shown in Fig. 1. Fig. 1a compares the different Waltz schemes. As observed for the residual coupling, the Waltz-17 CPD sequence performance degrades with increasing decoupler offset. For optimal decoupling the bandwidth is almost reduced by a factor of three compared to the Waltz-16. The introduction of an additional 90° pulse at the end of each supercycle might reduce the intensity of decoupling sidebands, but at the expense of a strongly reduced decoupling bandwidth. This first simple modification was therefore not pursued any longer. Waltz-64 and Waltz-65 both display similar decoupling bandwidths and gain, at identical decoupling conditions (pulse width & power level), approximately 10% greater decoupling bandwidth compared to the classical Waltz-16 sequence. This difference is not enormous (as expected from a rather simple modification) but still significant, as the efficiency of the decoupling is also more homogeneous over the decoupled bandwidth compared to Waltz-16. Fig. 1b allows for comparison between the most commonly used CPD sequences in high resolution NMR and the three Waltz schemes, "16", "64" and "65". Although GARP decoupling

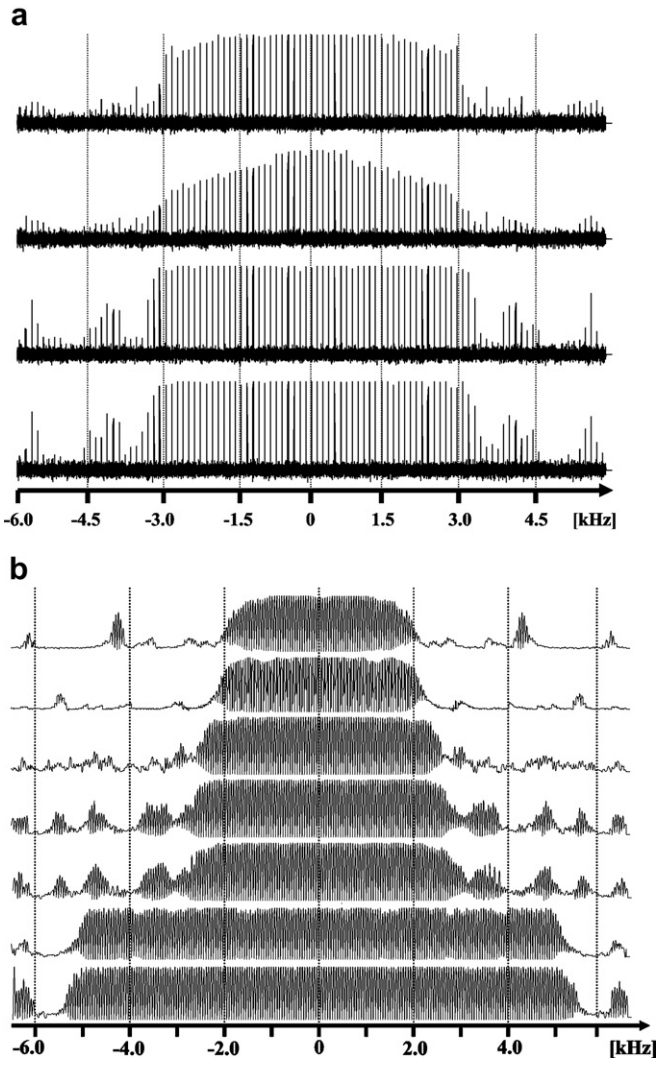

Fig. 1. Decoupling profiles acquired with a doped MeOH (^{13}C) sample. (a) Comparison of (from top to bottom) Waltz-16, Waltz-17, Waltz-64 and Waltz-65. Acquisition parameters: $\gamma B_2 = 3.125$ kHz, 128 decoupler offset steps, stepsize 100 Hz. (b) Comparison of (from top to bottom): DIPSI-2, MLEV-16, Waltz-16, Waltz-64, Waltz-65, Garp-1 and Garp-4 CPD decoupling schemes. Acquisition parameters: $\gamma B_2 = 2.5$ kHz, 256 decoupler offset steps, stepsize 50 Hz.

sequences do show a significant improvement in bandwidth they show typically increased linewidth of the decoupled carbon spectrum due to higher residual unresolved coupling.

The next step in assessing the performance of CPD sequences for ^{13}C polymer NMR applications was an analysis of the decoupling sidebands obtained. In order to understand which user accessible parameters influence the intensity and frequency of the decoupling sidebands, single scan spectra of the 40% dioxane sample were systematically acquired with varying decoupler offset and power level of decoupling. This was repeated twice, once keeping the decoupler power and pulse width constant, and once varying the power level and pulse width. An increase in the intensity of decoupling sidebands with increasing offset of the decoupler frequency with respect to the chemical shift of the decoupled spin was observed. Improper setting of the decoupling power level resulted in a dramatic increase in decoupling sideband intensity when applying lower power (more than 0.5 dB off), whereas using high power required more severe errors (more than 2 dB) to show increased decoupling sideband intensities. GARP sequences produce more intense and numerous visible decoupling sidebands compared to the Waltz decoupling schemes; therefore Waltz sequences are preferred for the quantitative ^{13}C NMR spectroscopy of most polymers including polyethylenes. The authors therefore decided to pursue further optimization of the Waltz sequences for ^{13}C NMR of polyethylene copolymers.

3.2. ^{13}C NMR of polyethylene with Waltz decoupling schemes

High quality ^{13}C NMR of polyethylene copolymers, which is essential for accurate quantification of copolymer composition and triad sequence distribution, requires very efficient proton decoupling. Inefficient decoupling can cause a loss of resolution and sensitivity. Some decoupling sequences can also generate artificial peaks which result in errors in results [17,18,27–29]. A HDPE sample was first used to explore several Waltz decoupling methods.

Fig. 2 is a schematic drawing of the HDPE sample used. Some carbons were labeled for ^{13}C NMR peaks assignments. This HDPE is a linear hydrocarbon containing small amount of long chain branching and some short chain branching from a butene comonomer. S_1, S_2 and S_3 represent the chain end carbons for long hydrocarbon chains; EEE represents the backbone CH_2 groups; x, y, n and m are integers; $1B_2$ and $2B_2$ are the side chain carbons of butene; α_n and β_n are the α and β carbons of the branch; SCB and LCB are the short and long chain branch methines, respectively.

Fig. 3 shows the ^{13}C NMR of sample A with three inverse gated decoupling pulse sequences, Waltz-16, Waltz-64 and Waltz-65. Peaks from sample A were identified with the labels shown in Fig. 2. A few small peaks between 30 and 40 ppm may come from unknown impurities. Waltz-16 is a periodic sequence of composite pulses, which requires only a modest amount of RF power and has good proton decoupling efficiency over reasonable bandwidths (Fig. 1). However, the periodic sequence has a long repetition period at low B_2 field and, as a consequence, decoupling sideband signals can be observed at integral multiples of the decoupler cycling rate, symmetrically disposed around the decoupled strong resonance signals. The higher the level of B_2 is, the faster the decoupler cycling rate and the weaker the cycling sidebands will be. In general, ^{13}C NMR of polyethylene copolymer has strong signals from the NMR solvents and from EEE sequence when the comonomer ratio is low. Although high decoupling power was used (decoupler 90° 60 μs), very strong decoupling sidebands which are labeled with asterisks were observed with Waltz-16 for sample

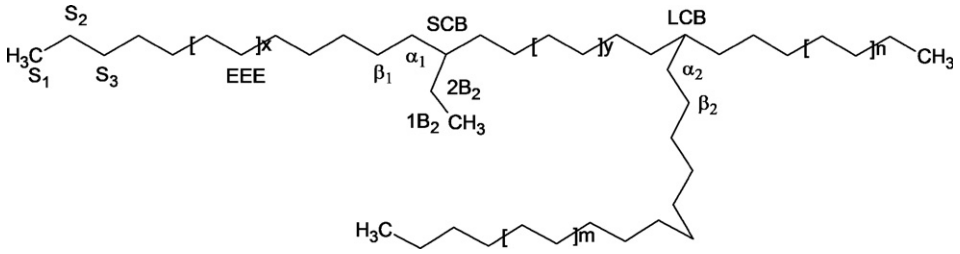

Fig. 2. A schematic drawing of the HDPE sample used.

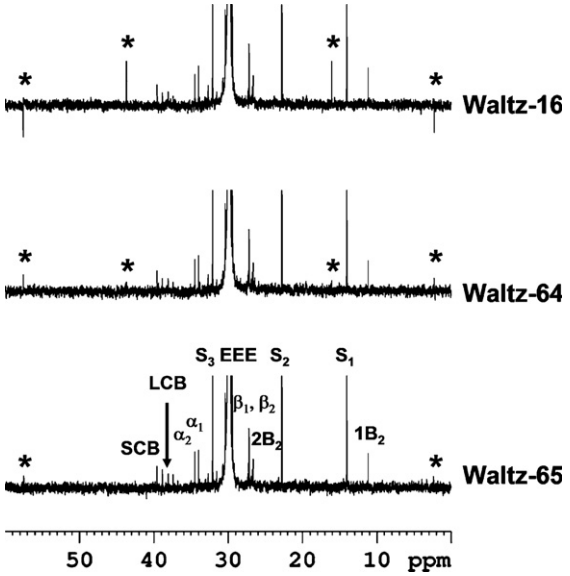

Fig. 3. ^{13}C NMR of sample A at 125 °C with Waltz-16, Waltz-64 and Waltz-65 decoupling. The S/N value for the peak at ca. 30 ppm is 15.8 k, 15.8 k and 16.0 k from top to bottom. Decoupling sidebands are labeled with (*). NS = 800.

A. These decoupling sidebands are in the chemical shift range of interest, for materials such as chlorinated polyethylene, chlorosulfonated polyethylene, poly(ethylene-co-propylene), poly(ethylene-co-propylene-co-5-ethylidene-2-norbonene), poly(ethylene-co-4-methyl-1-1pentene), poly (ethylene-co-norbornene), poly(ethylene-co-acrylic acid), poly (ethylene-co-methyl-acrylate), poly(ethylene-co-ethyl-acrylate), poly(ethylene-co-butyl acrylate) and poly(ethylene-co-methacrylic acid).

The Waltz-64 shows clearly improved performance with smaller decoupling sidebands, decoupling side bands are further reduced with Waltz-65, but still observable (Fig. 3). Therefore all three Waltz CPD sequences, Waltz-16, Waltz-64 and Waltz-65 are not very suitable for polyethylene copolymer ^{13}C NMR. TPPM15 was also tested. Although no decoupling sidebands were observed, the decoupling bandwidth was not broad enough to cover the chemical shift range of interest with the available decoupling power.

3.3. Reduction/elimination of decoupling sidebands

Reduction of the decoupling sideband intensities below detection with Waltz-65 could be achieved when using a different reference clock for the second (decoupler) channel with respect to the master clock of the spectrometer (data not shown). Following this result the next step was to "turn" the phase of the decoupling sidebands in a controlled fashion from scan to scan and finally achieve suppression of the most prominent decoupling sidebands. These phase steps can be achieved by starting the CPD supercycle at an increasing point in time from scan to scan (with respect to the pulse sequence timing). In order to decouple but still change the starting point of the CPD supercycle a bilevel implementation was used, where the CPD decoupling is split into two parts: the first part, increasing in length from scan to scan, is given with constant phase (hence "CW"), whereas the rest of the decoupled time is done in a synchronous CPD fashion.

In order to maintain sufficient decoupling bandwidth, the "CW" part is typically given with a fourfold power level. In polyolefin NMR decoupling power levels are typically already quite substantial, so the authors chose, in the first attempt, not to increase the power level for the "CW" part. Fig. 4 shows the first bilevel implementation bi_waltz-65_256, using a 256-step incrementation of the CW part. For quantitative study, decoupling power of Waltz-65 during d_1 was set to zero to avoid steady state NOE build up. Decoupling was started with a 165.6° pulse train which lasts for up to 23.5 ms (60 μs basic decoupler pulse length) and uses the same power as the subsequent Waltz-65. The decoupling must be started with a delay d_2, "predecoupling", which has to be longer than the CW pulse. This restricts the use of inverse gated decoupling experiments.

Fig. 5 shows the second implementation bi_Waltz-65_64pl, using a 64-step "CW" part, where the step size is divided by a factor of 2 and the power level for the CW part is changed by a factor of 4. Increasing the power level for the CW part and decreasing the total length of the first CW part allow this CPD method not only to be used with power gated but also with inverse gated decoupled experiments. In the latter method, the decoupler is turned on right after ^{13}C hard pulse. Decoupling is started with an 82.8° pulse train which lasts for up to 3.5 ms (60 μs basic decoupling pulse length) and uses four times the power than the subsequent Waltz-65.

The results of the ^{13}C NMR of sample A with bi_Waltz-65_256 and bi_Waltz_65_64pl decoupling are shown in Fig. 6. Two predecoupling times, 23.5 and 100 ms were used for the bi_Waltz-65_256. It can be seen that

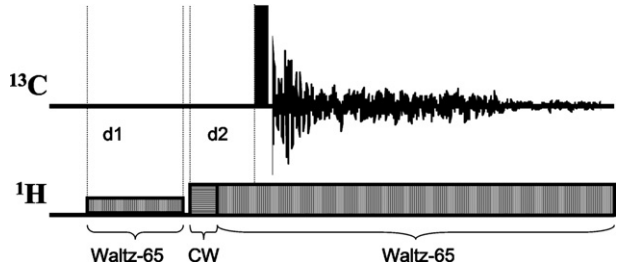

Fig. 4. Bi_waltz-65_256. 256-step "bilevel" implementation of Waltz-65 for power gated decoupling, $d_1 + d_2$ = relaxation delay. Decoupling starts with CW part (165.6° pulse), increasing from scan to scan until maximum length at 256th scan. Scan 257 is executed with same CW part as first scan.

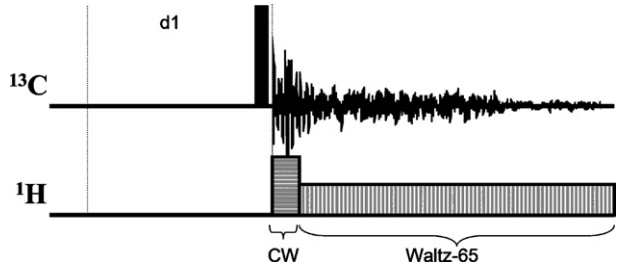

Fig. 5. Bi_Waltz_65_64pl. 64-step bilevel implementation of Waltz-65, d_1 = relaxation delay. Decoupling starts upon acquisition of the FID with CW part (82.8° pulse), increasing from scan to scan until maximum length at 64th scan. Scan 65 is executed with same CW part as first scan. The power of the applied CW part is 6 dB higher than the CPD part, to maintain the decoupling bandwidth.

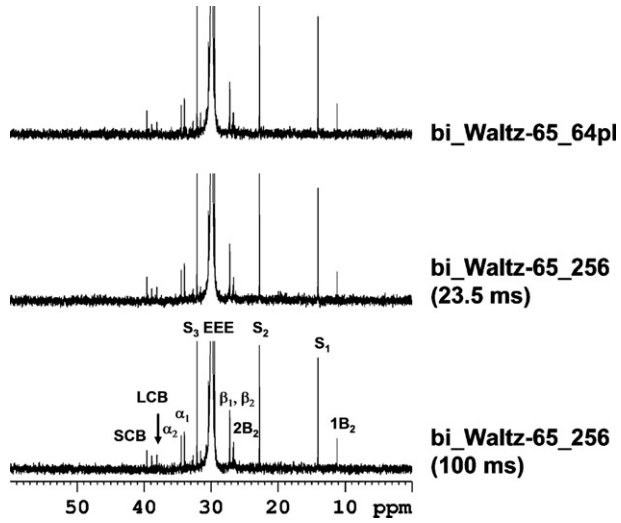

Fig. 6. ^{13}C NMR of sample A at 125 °C with bi_Waltz-65_256 (100 ms predecoupling), bi_Waltz-65_256 (23.5 ms predecoupling) and bi_Waltz-65_64pl decoupling. The S/N value for the peak at ca. 30 ppm is 16.8 k, 15.9 k and 16.6 k from top to bottom, NS = 800.

decoupling efficiencies were very good for both bi_Waltz-65_256 and bi_Waltz-65_64pl methods. No decoupling side bands were observed.

The bi_Waltz-65_256 and bi_Waltz-65_64pl methods were also applied to sample B. A schematic drawing of sample B (EO) is shown in Fig. 7. S_1, S_2 and S_3 represent the chain end carbons for long hydrocarbon chains; EEE represents backbone CH_2 groups; n and m are integers; $1B_6$ to $6B_6$ are side chain carbons of octene; α and β are α and β carbons of the branch carbon; Br is branch carbon of octene. For comparison, inverse gated decoupling pulse sequence Waltz-16, Waltz-64 and Waltz-65 were applied to this sample too.

Fig. 8 shows the 70 – 115 ppm region of the ^{13}C NMR of sample B with the inverse gated decoupling pulse sequence Waltz-16, Waltz-64 and Waltz-65. This is the region of interest for some polyethylene copolymers, such as chlorosulfonated polyethylene, poly(ethylene-co-vinyl acetate), poly(ethylene-co-vinyl alcohol) and oxidized polyethylene. Obviously, artificial peaks generated by Waltz-16, Waltz-64 and Waltz-65 decoupling may interfere with analysis.

The same region of NMR spectra of sample B obtained with bi_Waltz-65_256 and bi_Waltz-65_64pl methods is shown in Fig. 9. Two predecoupling times, 23.5 and 100 ms, were used for the bi_Waltz-65_256. No artificial peaks were observed with both bi_Waltz-65_256 and bi_Waltz-65_64pl methods.

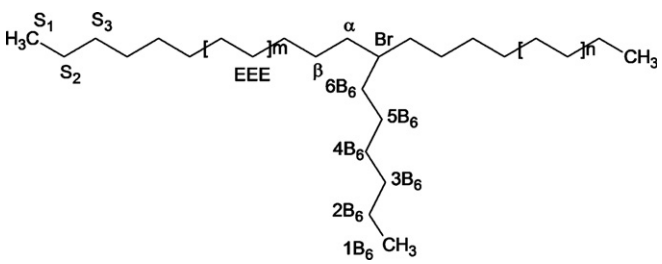

Fig. 7. A schematic drawing of poly(ethylene-co-1-octene).

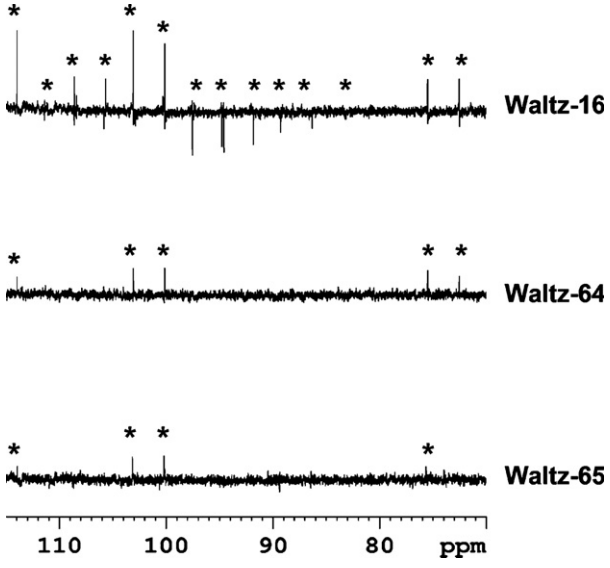

Fig. 8. ^{13}C NMR of sample B at 125 °C with Waltz-16, −64 and −65 decoupling. Artificial peaks are labeled with (*). NS = 8000.

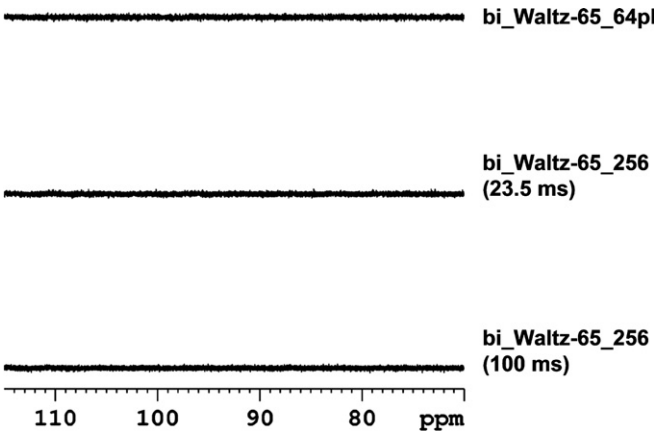

Fig. 9. ^{13}C NMR of sample B at 125 °C with bi_Waltz-65_256 (100 ms predecoupling), bi_Waltz-65_256 (23.5 ms predecoupling) and bi_Waltz-65_64pl decoupling, NS = 8000.

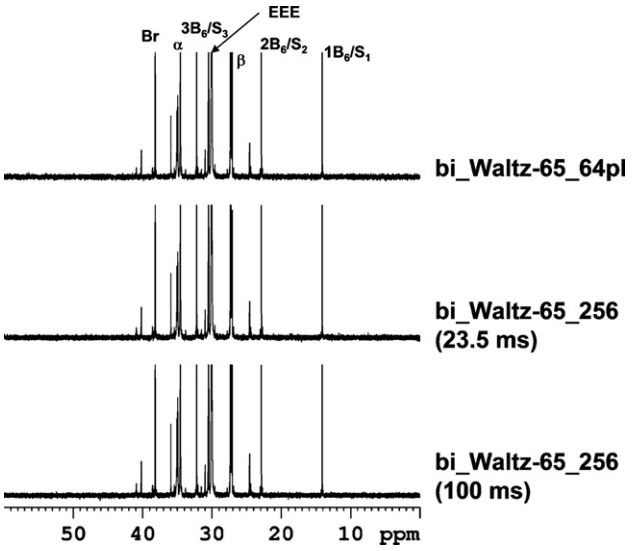

Fig. 10. ^{13}C NMR of sample B at 125 °C with bi_Waltz-65_256 (100 ms predecoupling), bi_Waltz-65_256 (23.5 ms predecoupling) and bi_Waltz-65_64pl decoupling. The S/N value for the peak at ca. 30 ppm is 7.2 k, 7.6 k and 8.1 k from top to bottom, NS = 8000.

NMR spectra from 0 to 60 ppm of sample B obtained with bi_Waltz-65_256 and bi_Waltz-65_64pl methods are shown in Fig. 10. Major peaks are identified with labels in Fig. 7. Due to the low natural abundance and small magnetogyric ratio of ^{13}C, a large number of scans are needed to get reasonable signal to noise ratio for composition and triad sequence distribution analysis of polyethylene copolymers. This results in very long experimental time for ^{13}C NMR analysis due to the relatively long T_1 values. In order to reduce T_1, $Cr(AcAc)_3$ was added to the sample [7–11]. It was initially believed that $Cr(AcAc)_3$ would eliminate unwanted NOE, especially if there is only 23.5–100 ms decoupling before ^{13}C hard pulse. Table 2 lists the integrals obtained from NMR spectra in Fig. 10. The integral for the $2B_6/S_2$ carbon was set to 100. It can be seen that bi_Waltz-65_256 generated larger integrals, which increased as the predecoupling time increased. The experimental data in Table 2 showed that NOE was still measurable even if very short predecoupling was used and substantial $Cr(AcAc)_3$ was present. Higher Cr^{3+} concentrations might reduce NOE further, but would result in loss of the resolution.

Based on the results and discussion above, the bi_Waltz-65_64pl method is the best method of those tested for acquiring high quality ^{13}C NMR data for composition and triad sequence distribution analysis of polyethylene copolymer. In addition, it requires no modification of pulse sequences or dataset setup procedures, only the CPD scheme needs to be switched. This should allow an easy and robust implementation for routine applications. Furthermore, data processing needs no modification.

3.4. Data analysis

At moderate field (for example, 400 MHz NMR) most of the ^{13}C NMR resonances of polyethylene copolymers are resolved sufficiently to allow assignments of carbon resonances down to the triad level. Copolymer composition and triad sequence distribution can be calculated with triad, Bernoulian, first order Markovian and second order

Table 2
^{13}C NMR integrals of sample B obtained with bi_Waltz-65_256 (23.5 and 100 ms predecoupling) and bi_Waltz-65_64pl methods

Chemical shift range (ppm)	Integrals with different decoupling methods			Integral increase compared with bi_Waltz-65_64pl (%)	
	Bi-Waltz-65_64pl	Bi-Waltz-65_256 (23.5 ms)	Bi-Waltz-65_256 (100 ms)	Bi-Waltz-65_256 (23.5 ms)	Bi-Waltz-65_256 (100 ms)
41.9–40.0	12.1	14.5	17.0	20	41
38.8–37.8	71.2	73.8	79.4	4	12
36.2–35.8	21.3	21.8	24.8	2	16
35.8–34.0	260.3	271.1	305.7	4	17
33.9–33.6	2.0	2.1	2.9	7	50
32.45–31.95	98.1	98.3	100.7	0	3
31.4–29.00	1224.8	1239.5	1300.7	1	6
28.0–26.7	242.6	249.4	269.7	3	11
25.0–24.2	9.9	11.0	12.8	12	30
23.12–22.63	100.0	100.0	100.0	0	0

Table 3
Composition and triads distribution of sample B obtained with bi_Waltz-65_256 (23.5 and 100 ms predecoupling) and bi_Waltz-65_64pl

	Composition and triads distribution		
	Bi-Waltz-65_64pl	Bi-Waltz-65_256 (23.5 ms)	Bi-Waltz-65_256 (100 ms)
C2 mol%	87.66	87.54	87.27
C8 mol%	12.34	12.46	12.73
C2 wt%	63.98	63.73	63.15
C8 wt%	36.02	36.27	36.85
EEE	0.677	0.672	0.662
EEO + OEE	0.188	0.190	0.194
OEO	0.012	0.013	0.016
OOO	0.003	0.002	0.000
OOE + EOO	0.028	0.028	0.028
EOE	0.092	0.094	0.099
Residual	3.3E-06	2.2E-06	4.9E-05

Markovian matrix methods which are more systematic, disciplined and reliable (O. D. Redwine, X. Qiu and Z. Zhou, to be published). The composition and triad sequence distribution of sample B shown in Fig. 10 are listed in Table 3. It can be seen that non-equal residual ^{1}H–^{13}C NOE generated with bi_Waltz-65_256 (23.5 and 100 ms predecoupling) resulted in unreliable results for composition and triad sequence distribution, for example, increased C8 mol%.

4. Conclusions

Modified Waltz, Waltz-64 and Waltz-65, decoupling schemes have been proposed with improved performance in both bandwidth and decoupling sideband intensity. They should preferably be used for any high resolution ^{13}C detect ^{1}H decoupled NMR experiments. The conditions required to acquire high quality quantitative ^{13}C NMR of polyethylene copolymer were discussed. Common decoupling sequences used in ^{13}C NMR of polymer samples, such as Waltz-16, generated decoupling sidebands, which may result in errors in composition and triad sequence distribution analyses. Other methods, such as TPPM15, have insufficient bandwidth and fail to effectively decouple all protons in polyolefin NMR, due to typical power restrictions from amplifiers and probes with high resolution NMR spectrometers. Modified Waltz CPD sequences, such as Waltz-64 and Waltz-65, do improve both bandwidth and sideband intensities, but decoupling sideband are still visible for polymers. The new decoupling method, bilevel Waltz-65 with a 64-step CW component, produces an artifact free spectrum for polyethylene copolymer composition and triad sequence distribution analyses.

Acknowledgments

The authors thank Ms. Cherry Hollis for sample preparation, Wolfgang Bermel and Detlef Moskau for continuous support and stimulating discussions, Janece Potter for lab and John G. DeCesare for instrument supports.

References

[1] M. De Pooter, P.B. Smith, K.K. Dohrer, K.F. Bennett, M.D. Meadows, C.G. Smith, H.P. Schouwenaars, R.A. Geerards, Determination of the composition of common linear low density polyethylene copolymers by carbon-13 NMR spectroscopy, J. Appl. Poly. Sci. 42 (1991) 399–408.
[2] J.C. Randall, A review of high-resolution liquid carbon-13 nuclear magnetic resonance characterizations of ethylene-based polymers, J. Macromol. Sci., Rev. Macromol. Chem. Phys. C29 (1989) 201–317.
[3] M.R. Seger, G.E. Maciel, Quantitative ^{13}C NMR analysis of sequence distributions in poly(ethylene-co-1-hexene), Anal. Chem. 76 (2004) 5734–5747.
[4] P.J. Adriaensens, F.G. Karssenberg, J.M. Gelan, V.B.F. Mathot, Improved quantitative solution state ^{13}C NMR analysis of ethylene-1-octene copolymers, Polymer 44 (2003) 3483–3489.
[5] W. Liu, P.L. Rinaldi, L.H. McIntosh, R.P. Quirk, Poly(ethylene-co-1-octene) characterization by high-temperature multidimensional NMR at 750 MHz, Macromolecules 34 (2001) 4757–4767.
[6] S. Berger, S. Braun, 200 and More NMR Experiments a Practical Course, Wiley-VCH Verlag GmbH & Co. KGaA, Weinheim, 2004, pp. 130.
[7] M.A. Villar, M.D. Failla, R. Quijada, R.S. Mauler, E.M. Valles, G.B. Galland, L.M. Quinzani, Rheological characterization of molten ethylene-a-olefin copolymers synthesized with Et[Ind]$_2$ZrCl$_2$/MAO catalyst, Polymer 42 (2001) 9269–9279.
[8] A.G. Simanke, G.B. Galland, L. Freitas, J. Alziro, H. Da Jornada, R. Quijada, R.S. Mauler, Influence of the comonomer content on the thermal and dynamic mechanical properties of metallocene ethylene/1-octene copolymers, Polymer 40 (1999) 5489–5495.
[9] G.B. Galland, R.S. Mauler, S.C. de Menezes, R. Quijada, ^{13}C-NMR study of ethylene/1-hexene and ethylene/1-octene copolymers obtained using homogeneous catalysts, Polym. Bull. (Berlin) 34 (1995) 599–604.
[10] J.V. Prasad, P.V.C. Rao, V.N. Garg, Quantification of branching in polyethylene by carbon-13 NMR using paramagnetic relaxation agents, Eur. Polym. J. 27 (1991) 251–254.
[11] R. Quijada, J. Dupont, M.S.L. Miranda, R.B. Scipioni, G.B. Galland, Copolymerization of ethylene with 1-hexene and 1-octene: correlation between type of catalyst and comonomer incorporated, Macromol. Chem. Phys. 196 (1995) 3991–4000.
[12] R.R. Ernst, Nuclear magnetic double resonance with an incoherent radio-frequency field, J. Chem. Phys. 45 (1966) 3845–3861.
[13] M.H. Levitt, R. Freeman, Composite pulse decoupling, J. Magn. Reson. 43 (1981) 502–507.
[14] M.H. Levitt, R. Freeman, T. Frenkiel, Broadband heteronuclear decoupling, J. Magn. Reson. 47 (1982) 328–330.
[15] M.H. Levitt, R. Freeman, T. Frenkiel, Supercycles for broadband heteronuclear decoupling, J. Magn. Reson. 50 (1982) 157.
[16] M.H. Levitt, R. Freeman, T. Frenkiel, Broadband decoupling in high-resolution NMR spectroscopy, Adv. Magn. Reson. 11 (1983) 47–110.
[17] A.J. Shaka, J. Keeler, T. Frenkiel, R. Freeman, An improved sequence for broadband decoupling: WALTZ-16, J. Magn. Reson. 52 (1983) 335–338.
[18] A.J. Shaka, J. Keeler, R. Freeman, Evaluation of a new broadband decoupling sequence: WALTZ-16, J. Magn. Reson. 53 (1983) 313–340.
[19] A.J. Shaka, P.B. Barker, R. Freeman, Computer-optimized decoupling scheme for wideband applications and low-level operation, J. Magn. Reson. 64 (1985) 547–552.
[20] A.J. Shaka, J. Keeler, Broadband spin decoupling in isotropic liquids, Prog. NMR Spectrosc. 19 (1987) 47–129.

[21] Z. Starcuk Jr., K. Bartusek, Z. Starcuk, Heteronuclear broadband spin-flip decoupling with adiabatic pulses, J. Magn. Reson. A. 107 (1994) 24–31.
[22] M.R. Bendall, Broadband and narrowband spin decoupling using adiabatic spin flips, J. Magn. Reson. A 112 (1995) 126–129.
[23] E. Kupce, R. Freeman, Optimized adiabatic pulses for wideband spin inversion, J. Magn. Reson. A 118 (1996) 299–303.
[24] R. Fu, G. Bodenhausen, Evaluation of adiabatic frequency-modulated schemes for broadband decoupling in isotropic liquids, J. Magn. Reson. A 119 (1996) 129–133.
[25] A.E. Bennett, C.M. Rienstra, M. Auger, K.V. Lakshmi, R.G. Griffin, Heteronuclear decoupling in rotating solids, J. Chem. Phys. 103 (1995) 6951–6958.
[26] Y.Y. Yu, B.M. Fung, An efficient broadband decoupling sequence for liquid crystals, J. Magn. Reson. 130 (1998) 317–320.
[27] A.J. Shaka, P.B. Barker, C.J. Bauer, R. Freeman, Cycling sideband in broad-band decoupling, J. Magn. Reson. 67 (1986) 396–401.
[28] E. Kupce, R. Freeman, G. Wider, K. Wuthrich, Suppression of cycling sidebands using bi-level adiabatic decoupling, J. Magn. Reson. A 122 (1996) 81–84.
[29] R.W. Dyksstra, A method to suppress cycling sidebands in broadband decoupling, J. Magn. Reson. 82 (1989) 347–351.
[30] S. Zhang, D. Gorenstein, Adiabatic decoupling sidebands, J. Magn. Reson. 144 (2000) 316–321.